

Simplified Calculation Approach of Load-Deformation Relationships of a Beam-Column Element

Ercan YÜKSEL^{1*}, Faruk KARADOĞAN¹

¹ Istanbul Technical University, Faculty of Civil Engineering, 34469, Maslak-Istanbul, TURKEY

Received: 17.02.2009 Revised: 11.05.2009 Accepted: 11.05.2009

ABSTRACT

A simple algorithm for the derivation of load-deformation relationships of a beam-column element is developed. Nonlinear beam-column element is modeled considering inelastic flexural deformations, geometric nonlinearities and elastic shear and axial deformations. In a frame structure, one element is used for one member that may be loaded by distributed loads. The distribution of inelasticity along the member is taken into consideration. The algorithm can be used not only in nonlinear static analysis but also calculation of the elastic stiffness characteristics of non-prismatic members such as haunches and tapered beams. Correlation studies with the existing literature have been conducted with the objective to establish the validity of the proposed algorithm.

Key Words: *Beam-column element; inelastic deformations; spread plasticity; stiffness characteristics; nonlinear static analysis.*

1. INTRODUCTION

Definition of the load-deformation relationships of a beam-column element is an important step in nonlinear static analysis. Simplicity, reliability and computational effectiveness are the most important features of beam-column elements. A simplified calculation approach for the derivation of load-deformation relationships of a beam-column element is presented in this study. Although the proposed algorithm is very simple compared with the existing formulation in the literature, it is able to produce satisfactory results. The proposed algorithm has been implemented in a computer program named *DOC2B*, [1], which is an analytical tool used for the performance analyses of frame type structures. The proposed algorithm can also be used to calculate the elastic stiffness matrix of non-prismatic members such as haunches and tapered beams. The efficiency of the developed algorithm is demonstrated by giving numerical examples.

Since inelastic deformations are distributed along the members rather than being concentrated at critical sections, a more accurate description of the inelastic behavior is possible with the distributed nonlinearity models, [2]. Earlier beam-column models consist of two cantilever elements that are connected at the fixed point of contra-flexure of the member, [3], [4]. Umemura *et al.* [4] used continuous function to represent the

variation of rigidity along the member length. Takayanagi *et al.* [5] proposed to divide the element into a finite number of short longitudinal elements, each represented by a nonlinear rotational spring. The static condensation is used to reduce this multi-spring model to a single beam-column element. Filippou *et al.* [6] identified the lengths over which the moment M exceeds the corresponding yield value, with length z_i and z_j .

Assuming an average rigidity of all sections within z_i and z_j , flexibility matrix of the member is formulated. Valles *et al.* [7] produced a beam-column element which is a basic three-dimensional space frame element considering flexural, shear and axial deformations, and it has been implemented in various versions of IDARC. Izzuddin *et al.* [8] proposed a new beam-column formulation modeling of three dimensional RC frames. The formulation is intended for modeling the nonlinear elastic behavior of a whole RC beam-column with only one element. It presents the element formulation in a local Eulerian system where the cross section response over the element length is transformed into local element forces and tangent stiffness. Taylor *et al.* [9] developed some solutions for Euler-Bernoulli and Timoshenko theories of beams in which material behavior may be elastic and inelastic. The local constitutive equations are integrated over the beam cross section to obtain the relations for beam

*Corresponding author, e-mail: yukselerc@itu.edu.tr

resultants. The approach leads to a shear deformable formulation that is free of locking effects. Nanokorn [10] proposed a new two-dimensional, two noded beam-column element for the inelastic analysis of plane frames. It is capable of having multiple internal hinges whose positions are not limited to the ends of the beam-column element. It is possible to use one element for one member of a frame structure even when distributed loads are present.

2.2. Primary Element

The simplified calculation approach is aimed at representing a whole inelastic member with one element. A member is divided into finite number of segments along its length so the spread of inelasticity

can be modeled more accurately. The primary element is chosen as a cantilever beam that is to be of length L . Rigid end offsets may be available at both ends. The primary element consists of N_{seg} segments for which the flexural characteristics are assumed to be constant. It is divided into k_{max} small segments of length ΔL_k to apply the proposed recurrence equations, Eq. (1) and Figure 1.

$$\Delta L_s = \frac{L}{N_{seg}} \quad \Delta L_k = \frac{L}{k_{max}} \quad (1)$$

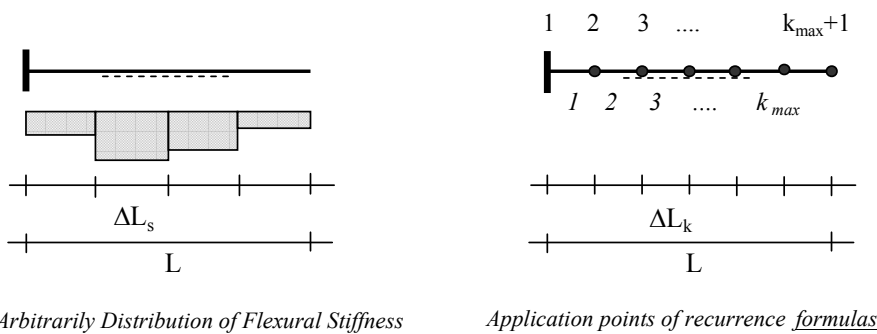


Figure 1. Definition of the small segments.

P_1, P_2, P_3 are independent end forces and q is uniformly distributed span loading of the primary element. The bending moments obtained from the unit independent end forces and distributed span loading are named as M_1, M_2, M_0 , respectively, Figure 2. The

end displacements arise from the unit end forces and distributed span loading are depicted as $\overline{f}_{11}, \overline{f}_{12}, \overline{f}_{21}, \overline{f}_{22}, \overline{f}_{10}, \overline{f}_{20}$.

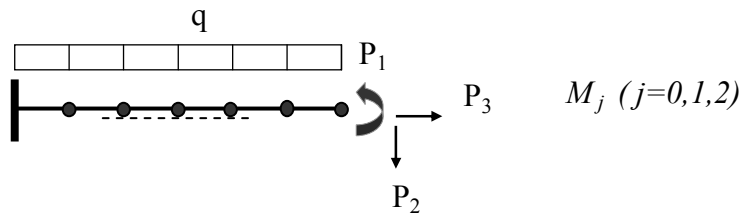


Figure 2. Independent end forces and uniformly distributed span loading.

Two recurrence equations which are suitable for quick calculation have been produced to obtain the deflected shapes of the primary element.

2.3. Rotation Difference between Successive Points

As shown in Figure 3, a pair of unit moments \overline{M} is moved from the fix support to the free end of the primary element. The equation written by virtual work theory to calculate the rotation difference between

successive points is called as *rotation difference equation* and given in Eq. (2). In this equation, M_j shows the moments obtained from the unique values of independent end forces, EI_k is average flexural stiffness of k^{th} segment of the primary element, Eq. (3). M_k^L and M_k^R correspond moments at the end sections of the k^{th} segment, Figure 4.

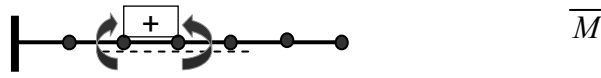


Figure 3. A pair of unit moments.

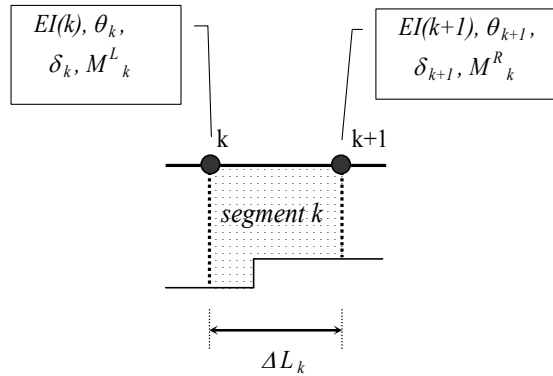


Figure 4. k^{th} segment of the primary element.

$$\Delta\theta_k = \int \frac{M_j \bar{M}}{EI_k} ds = \frac{M_k^L + M_k^R}{2} * 1 * \frac{\Delta L_k}{EI_k} + \frac{2}{3} * \Delta L_k * 1 * q * \Delta L_k^2 * \frac{1}{8EI_k}$$

$$j = 0, 1, 2 \quad k = 1, k_{\max} + 1 \quad (2)$$

$$EI_k = \frac{EI(k) + EI(k+1)}{2} \quad (3)$$

Using the boundary condition $\theta_1 = 0$ at the fix support and Eq. (4), the absolute rotation at each point of the primary element can be calculated, successively.

$$\theta_{k+1} = \theta_k + \Delta\theta_k \quad ; \quad k = 1, \dots, k_{\max} + 1 \quad \dots \quad (4)$$

2.4. Transversal Displacement

$$-M_k^L = M_{0k}^L + m_{k\theta_k}^k \theta_k + m_{k\theta_{k+1}}^k \theta_{k+1} + m_{\delta}^k (\delta_{k+1} - \delta_k) \quad ; \quad k = 1, \dots, k_{\max} + 1 \quad (5)$$

For uniformly distributed load, q , fixed-end moment is calculated using Eq. (6) as:

$$M_{0k}^L = \frac{q\Delta L_k^2}{12} \quad (6)$$

The transverse displacement at each points of the primary element can be calculated, using Eq. (7) which is called as *Transverse Displacement Equation*.

$$\delta_{k+1} = \frac{1}{m_{\delta}^k} \left(-M_k^L - \frac{q\Delta L_k^2}{12} - m_{k\theta_k}^k \theta_k - m_{k\theta_{k+1}}^k \theta_{k+1} + m_{\delta}^k \delta_k \right) \quad ; \quad k = 1, k_{\max} + 1 \quad (7)$$

The forces at the ends of the segments due to unit rotation and translation are calculated using Eq. (8).

$$m_{k\theta_k} = \frac{4EI_k}{\Delta L_k} \quad m_{k\theta_{k+1}} = \frac{2EI_k}{\Delta L_k} \quad m_\delta = \frac{6EI_k}{\Delta L_k^2} \quad (8)$$

2.5. Shear Deformations

Shear deformations are to be considered elastically. The forces due to the unit rotation and translation are calculated using Eq. (9).

$$m_{k\theta_k} = \frac{4EI_k}{\Delta L_k} \frac{1+c}{1+4c} \quad m_{k\theta_{k+1}} = \frac{2EI_k}{\Delta L_k} \frac{1-2c}{1+4c} \quad m_\delta = \frac{6EI_k}{\Delta L_k^2} \frac{1}{1+4c} \quad (9)$$

where

$$c = \frac{3EI_k}{\Delta L_k^2 GF'} \quad (10)$$

G is shear modulus of elasticity, F' is effective shear area of cross section in Eq. (10).

2.6. Second Order Effect of Axial Force

For k^{th} segment of the primary element, additional shear forces due to the second order effect of axial force are calculated. Relative transverse displacement and

axial force of the segment are multiplied and the result is divided to the segment length as shown in Figure 5 and given in Eq. (11).

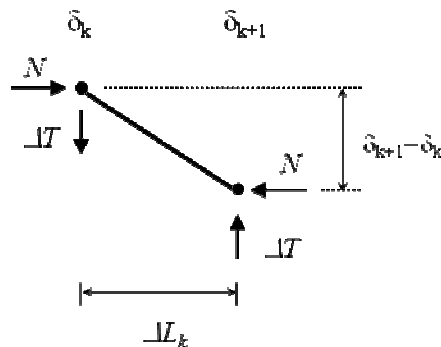


Figure 5. Calculation of the second order shear forces on a segment of the primary element.

$$\Delta T = \frac{(\delta_{k+1} - \delta_k)N}{\Delta L_k} \quad (11)$$

The calculated second order shear forces are added to the applied loading for both of the *rotation difference* and *transverse displacement equations*. An iterative process is applied until the results of successive steps converge.

2.7. Stiffness Matrix of Primary Element

The end displacements of the primary element $\overline{f}_{11}, \overline{f}_{12}, \overline{f}_{21}, \overline{f}_{22}, \overline{f}_{10}, \overline{f}_{20}$ are calculated using developed recurrence equations. The corresponding flexural stiffness matrix is calculated by a simple inversion of the flexibility matrix using Eq. (12). The end forces of \overline{P}_{01} and \overline{P}_{02} are calculated using Eq. (12).

$$\begin{bmatrix} \overline{f} \end{bmatrix} = \begin{bmatrix} \overline{f}_{11} & \overline{f}_{12} \\ \overline{f}_{21} & \overline{f}_{22} \end{bmatrix} \quad \begin{bmatrix} \overline{k} \end{bmatrix} = \begin{bmatrix} \overline{k}_{11} & \overline{k}_{12} \\ \overline{k}_{21} & \overline{k}_{22} \end{bmatrix} = \begin{bmatrix} \overline{f} \end{bmatrix}^{-1}$$

$$\overline{P}_{01} = -(\overline{k}_{11} * \overline{f}_{10} + \overline{k}_{12} * \overline{f}_{20}) \quad \overline{P}_{02} = -(\overline{k}_{12} * \overline{f}_{10} + \overline{k}_{22} * \overline{f}_{20}) \quad (12)$$

2.8. Definition of Sectional Flexural Stiffness

The gradient of the moment-curvature relation corresponds to *the flexural stiffness* which includes all the sectional properties in a typical loading condition. Given the distribution of flexural stiffness along the span of a beam-column element, element flexibility matrix can be calculated easily using the proposed algorithm for the elastic as well as inelastic stage of its

response. *Initial secant stiffness* is used for the definition of sectional stiffness as shown in Figure 6. M_s^c is the flexural moment obtained for the section by using the previous step's sectional stiffness of EI_s^o . M_s^d is the moment corresponding to the curvature of $\chi_s = M_s^c / EI_s^o$. EI_s^n is sectional stiffness to be used in the next step of the analysis and it is calculated as $EI_s^n = M_s^d / \chi_s$.

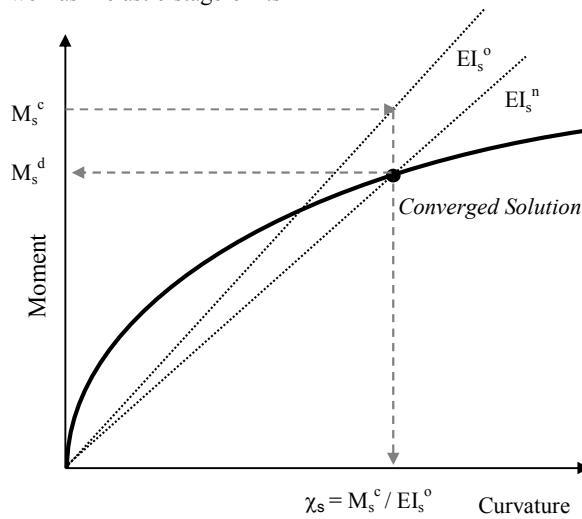


Figure 6. Linearization on axial force dependent moment-curvature diagram.

The algorithm performs successive linear solutions to satisfy the sectional moment-curvature relationships. If a convergence criterion is not satisfied, the stiffness and loading matrices are updated, and a new solution is to be attempted. This iterative procedure continues until the problem converges. Although the convergence speed of initial secant stiffness method is relatively slow, it guaranties not to have any singularity or convergence problems.

3. COMPARISON STUDIES

3.1. Example 1

Banerjee [11] used Bernoulli-Euler theory and Bessel functions to obtain explicit expressions for the exact static stiffness for axial, torsion and flexural deformation of an axially loaded tapered beam-column element. The calculated stiffness coefficients of the tapered beam-column element that carries a compressive axial load of $0.80 P_{cr}$ where P_{cr} is the lowest critical buckling load with both ends clamped are compared with the results of the developed algorithm. Eq. (13) shows the definition of sectional properties.

$$\begin{aligned}
 A(x) &= A_g \left(1 + c \frac{x}{L} \right)^l \\
 I(x) &= I_g \left(1 + c \frac{x}{L} \right)^{n+2}
 \end{aligned}
 \tag{13}$$

where c is a constant such that $c > -1$, L is the length of the beam-column element, x is the distance from one end of the beam, l can have any value and n is 1, 2 or -1 . The geometrical and mechanical properties of the beam-column element are as follows: Length of the element is $L = 5$ m., axial and flexural rigidity of the g section is $EA_g = 2.8 \cdot 10^6$ N, $EI_g = 1759.29$ Nm^2 , respectively. An axial compression force of $0.8 P_{cr}$ is used where $P_{cr} = 8077.8$ N, and c , l and n parameters are all equal to 1.0.

For solution of the problem with the developed algorithm, beam-column element is divided into 10 sub-elements and different values for N_{seg} and k_{max} have been tried to evaluate sensitivity of the results. The "exact solution" proposed by Banerjee is given in Column 1 of Table 1. For the case where $N_{seg} = 4$ and $k_{max} = 20$, the biggest relative difference between calculated and "exact values" is 0.611%. Relative differences in the case of $N_{seg} = 40$ and $k_{max} = 200$ are given in Column 4 of Table 1 and the biggest relative difference decreases to 0.014%. Lastly, it is checked the effect of large values like $N_{seg} = 400$ and $k_{max} = 800$ and it is obtained that the biggest relative difference is about 0.008%. The

numerical solutions for the different values of N_{seg} and k_{max} parameters approach the “exact solution” given by Banerjee. It is obvious that the proposed algorithm converges to a unique solution.

3.2. Example 2

A RC portal frame is chosen to make comparison between the results of developed algorithm and OpenSees [12] which is an object oriented framework for finite element analysis. Although only material type nonlinearity is used in the first analysis, material and geometric type nonlinearities are considered together in the second analysis. The geometry and cross sectional

properties of the system are given in Figure 7. The constant vertical loads acting on columns are 600 kN.

All of beam and column elements of the system have the same cross section and reinforcing details. The total area of longitudinal reinforcement in the typical cross section is equal to 25.806 cm² and it is uniformly distributed in the cross section. Constitutive models for well confined concrete and steel reinforcement are shown in Figure 8. For the sake of simplicity, a unique concrete model is defined for whole section. Moment curvature relationships are depicted in Figure 9 for two different axial force levels.

Table 1. Comparing the results of alternative solutions.

Stiffness Coefficients	“Exact Solution”	$N_{seg} = 4$ $k_{max} = 20$	$N_{seg} = 40$ $k_{max} = 200$	Relative Difference ($\times 10^{-5}$)	$N_{seg} = 400$ $k_{max} = 800$
	(1)	(2)	(3)		(4)
$K_{66} = K_{44} = K_{64}$	1231.588	1231.157	1231.576	0.97	1231.581
$K_{61} = K_{14}$	951.565	949.764	951.534	3.26	951.552
$K_{62} = K_{42}$	647.259	643.302	647.168	14.06	647.210
K_{11}	4374.018	4367.367	4373.806	4.85	4373.878
K_{12}	9131.843	9116.189	9131.476	4.02	9131.640
K_{22}	12368.139	12332.698	12367.319	6.63	12367.687

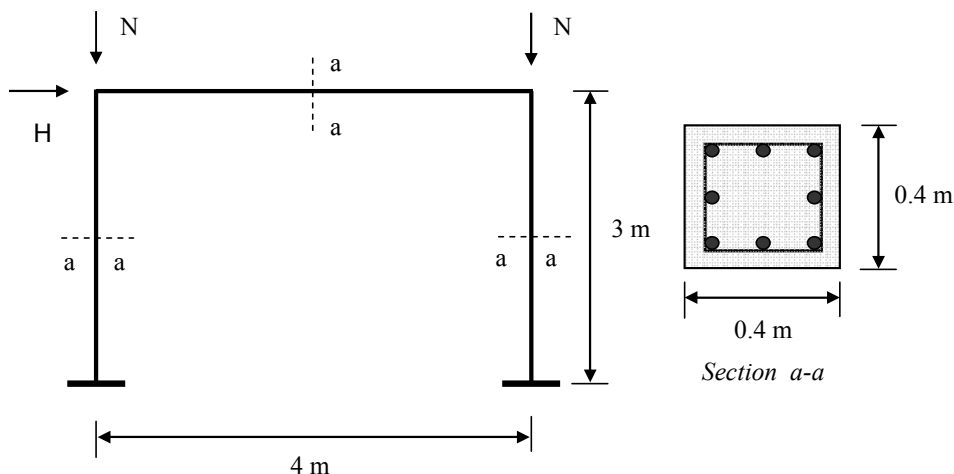


Figure 7. Geometry and typical cross section of the system.

The nonlinear beam-column element which considers the spread of plasticity along the element has been used in OpenSees in which RC cross sections are divided into a mesh 30 by 30. Total number of the integration points along the frame elements is set to 10. Linear elastic axial stiffness is defined for all the frame

elements. The lateral top displacement versus base shear relationships obtained by *DOC2B* and OpenSees are given together, in Figure 10. Comparisons of the results show that the proposed algorithm is in a good agreement with OpenSees.

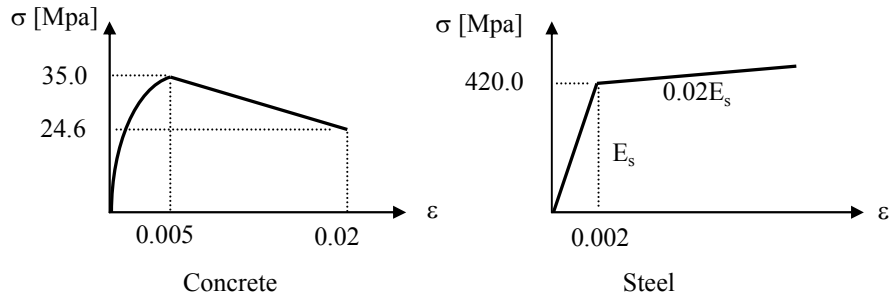


Figure 8. Confined concrete and steel constitutive models.

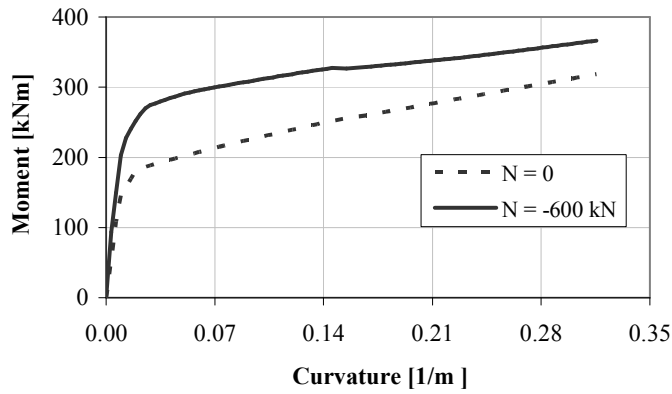


Figure 9. Moment-curvature relationships.

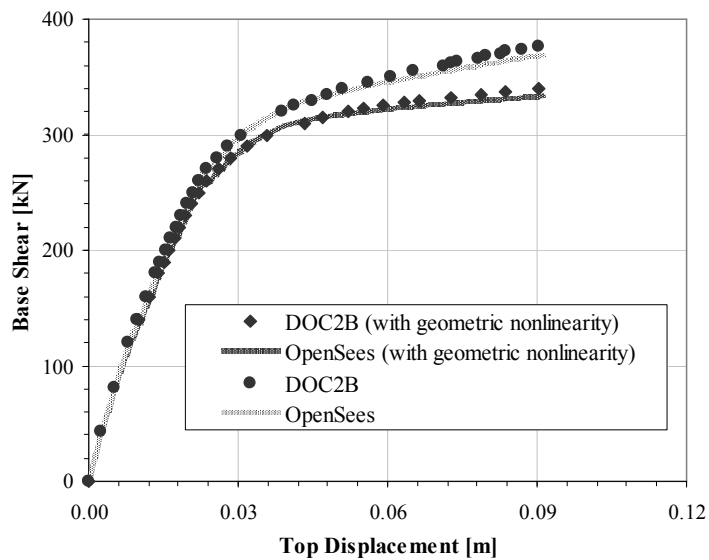


Figure 10. Base shear top displacement relationships.

The lateral top displacement and bending moment at the bottom section of right column of the frame

corresponding to 360 kN base shear are compared in

Table 2, for different values of N_{seg} and k_{max}

parameters in the developed algorithm.

Table 2. Some comparisons for Example 2.

Some Quantities	$N_{seg} = 10$	$N_{seg} = 40$	$N_{seg} = 100$	$N_{seg} = 400$
	$k_{max} = 20$	$k_{max} = 200$	$k_{max} = 200$	$k_{max} = 800$
Lateral Top Disp. [m]	0.06175	0.06944	0.07120	0.07131
Bending Moment [kNm]	333.55	333.36	333.34	333.29

3.3. Example 3

A portal frame with an inclined member shown in Figure 11 is chosen as a third example, [10]. An uniformly distributed load, q , is applied to *element #2* of the

portal frame. The problem is solved by using three beam-column elements. Perfectly plastic behavior is assumed for all of the elements. The required properties such as initial flexural stiffness EI and the plastic moment capacity M_p are assumed to be same for each element.

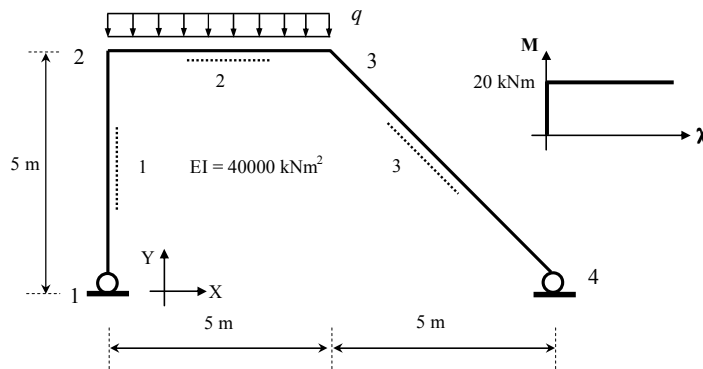


Figure 11. Geometry of the portal frame and moment-curvature relationship.

Horizontal displacement at *point #2* versus uniformly distributed load intensity q relationship obtained from *DOC2B* is drawn in Figure 12. Critical values of this graph are exactly same with the values given in [10].

Figure 13 demonstrates graphically the distribution of secant stiffness, EI , along the portal frame for the last step of the analysis. Lower stiffness values are reached at the near vicinity of *point #2* and the section that is

3.75 m away from the left end of *element #2*. These are exactly same locations with the plastic hinges defined in [10]. Plastic zone lengths can be extracted from the developed algorithm. One of the important advantages of the developed algorithm is to use one element for one member even loaded with distributed load.

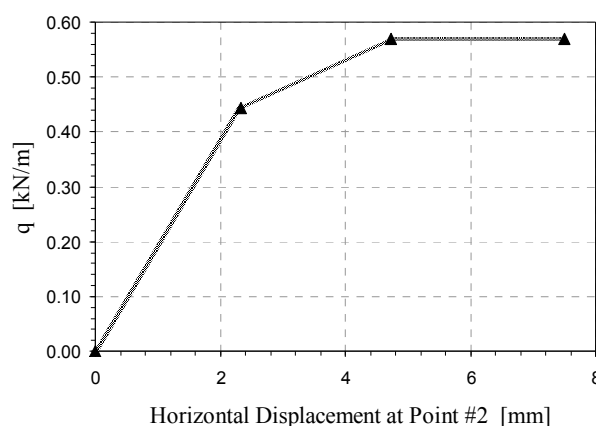


Figure 12. Distributed Load vs. Lateral Displacement of the Frame.

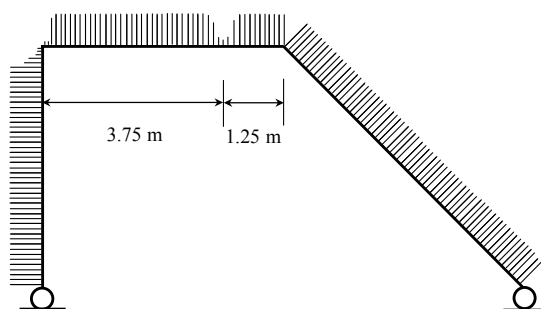


Figure 13. Load-response curve and distribution of flexural stiffness.

4. SUMMARY AND CONCLUSIONS

This research work presents a simple alternative algorithm for the derivation of load-deformation relationships of a beam-column element. The proposed algorithm which is very simple, reliable and computationally effective, can be used for analysis of non-prismatic members and nonlinear static analysis of frame type structures subjected to monotonic loads. Several applications illustrating the use of the nonlinear element were given.

The main features of the algorithm are those (i) one element is used for one member, (ii) the solution satisfies all equilibrium equations, (iii) the spread of inelasticity is considered along member length.

The comparative examples show that optimal values for N_{seg} and k_{max} parameters in the developed algorithm can be set as 40 and 200, respectively. The implementation of the developed algorithm in the computer program *DOC2B* for the nonlinear static analysis of large structures is presently completed and Example 2 is prepared using this program. The examples of computations made have proved effectiveness and correctness of the proposed algorithm.

REFERENCES

- [1] Yuksel E., "Nonlinear Analysis of 3D Large Structures with Certain Irregularities", 1998, Ph.D. Thesis, submitted to Graduate Scholl of ITU, (in Turkish) (1998).
- [2] Park R., Kent D., Sampson R., "Reinforced Concrete Members with Cyclic Loading", *Journal of Structural Engineering*, 98: 1341-1360 (1972).
- [3] Otani S., "Inelastic Analysis of R/C Frame Structures", *ASCE Journal of the Structural Division*, 100: 1433-1449 (1974).
- [4] Umemura H., Aoyama H., Takizawa H., "Analysis of the Behavior of R/C Structures During Strong Earthquake Based on Empirical Estimation of Inelastic restoring Force Characteristics of Members", *Proceedings of the Fifth World Conference on Earthquake Engineering*, Vol.2, Italy (1974).
- [5] Takayanagi T., Schnobrich W.C., "Computed Behavior of Reinforced Concrete Coupled Shear Walls", *Structural Research Series No.434*, Civil Engineering Studies, University of Illinois, Urbana, Illinois (1976).

- [6] Filippou F.C., Issa A., “Nonlinear Analysis of Reinforced Concrete Frames under Cyclic Load Reversals”, *Rep.No.UCB/EERC-88/12*, Earth. Eng. Res. Center, University of California, Berkeley (1988).
- [7] Valles, R.E., Reinhorn AM, Kunnath, SK, Li C, Madan A. , “IDARC2D Version 4.0: A Computer Program for the Inelastic Damage Analysis of Buildings”, *Technical Report MCEER-96-0010*. Department of Civil, Structural and Environmental Engineering, State University of New York at Buffalo (1996).
- [8] Izzuddin B.A., Siyam A.A.F.M., Lloyd Smith D., “An efficient beam-column formulation for 3D reinforced concrete frames”, *Computer and Structures*, 80: 659-676 (2002).
- [9] Taylor R.L., Filippou F.C., Saritas A., Auricchio F., “A mixed finite element method for beam and frame problems”, *Computational Mechanics*, 31: 192-203 (2003).
- [10] Nanakorn P., “A two dimensional beam-column finite element with embedded rotational discontinuities”, *Computer and Structures*, 82: 753-762 (2004).
- [11] Banerjee J.R., “Exact Bernoulli-Euler Static Stiffness Matrix for A Range of Tapered Beam-Columns”, *Int. J. for Num. Meth. in Eng.*, 23: 1615-1628 (1986).
- [12] OpenSees, “Open System for Earthquake Engineering Simulation”, *Pacific Earthquake Engineering Research Center*, (2005).